nature geoscience

LETTERS

PUBLISHED ONLINE: 6 NOVEMBER 2011 | DOI: 10.1038/NGEO1301

Abundant Early Palaeogene marine gas hydrates despite warm deep-ocean temperatures

Guangsheng Gu[1]*, Gerald R. Dickens[2,3]*, Gaurav Bhatnagar[1]†, Frederick S. Colwell[4], George J. Hirasaki[1] and Walter G. Chapman[1]

Abrupt periods of global warming between 57 and 50 million years ago—known as the Early Palaeogene hyperthermal events—were associated with the repeated injection of massive amounts of carbon into the atmosphere[1–4]. The release of methane from the sea floor following the dissociation of gas hydrates is often invoked as a source[5]. However, seafloor temperatures before the events were at least 4–7 °C higher than today[1], which would have limited the area of sea floor suitable for hosting gas hydrates[6,7]. Palaeogene gas hydrate reservoirs may therefore not have been sufficient to provide a significant fraction of the carbon released. Here we use numerical simulations of gas hydrate accumulation[8] at Palaeogene seafloor temperatures to show that near-present-day values of gas hydrates could have been hosted in the Palaeogene. Our simulations show that warmer temperatures during the Palaeogene would have enhanced the amount of organic carbon reaching the sea floor as well as the rate of methanogenesis. We find that under plausible temperature and pressure conditions, the abundance of gas hydrates would be similar or higher in the Palaeogene than at present. We conclude that methane hydrates could have been an important source of carbon during the Palaeogene hyperthermal events.

Earth's surface, including deep ocean water, was generally 5–9 °C warmer in the late Palaeocene and early Eocene relative to the present day, presumably because of much higher atmospheric p_{CO_2} (ref. 1). During a long-term warming trend within this interval, at least two and probably more 'hyperthermals' occurred. These were geologically brief (<200 kyr) events characterized by intense global warming, profound environmental change and massive input of ^{13}C-depleted CO_2 (refs 2–4). The Palaeocene–Eocene Thermal Maximum (PETM) at about 56 million years (Myr) ago is the most pronounced and best-documented example. In this case, seafloor temperature (T_{sf}) rose an additional ~5 °C within 50 kyr (refs 1,9–12). Nearly coeval with the warming, at least 2,000 gigatons (Gt) of ^{13}C-depleted carbon entered the ocean and atmosphere[1,6]. This is evidenced by a significant (>2‰) decrease in the δ^{13}C value of carbon-bearing material deposited during the onset of the PETM, and coincident dissolution of carbonate in deep-sea environments[9–13].

The carbon injections of the PETM and other hyperthermals challenge conventional models for global carbon cycling[1,5]. A widely discussed cause has been thermal perturbation of a large gas hydrate capacitor[5,6]. As for the present day, the upper hundreds of metres of marine sediments hosted highly ^{13}C-depleted CH_4 ($\delta^{13}C < -50$‰) as gas hydrate[14]. At steady state, a portion of organic carbon buried in sediment was converted to CH_4, much of this CH_4 was stored as gas hydrate, and a small portion of carbon returned to the ocean through anaerobic oxidation in shallow sediment. However, when T_{sf} rose, large quantities of gas hydrate converted to free gas, and the output of ^{13}C-depleted CH_4 from the sea floor increased substantially, presumably through venting or sediment failure. Once released, the CH_4 was oxidized to CO_2 in the ocean (through microbial activity), the atmosphere or both.

Recent studies of sedimentary records across the PETM are consistent with widespread CH_4 release from submarine gas hydrates during this time[5,15]. In particular, environmental changes, including ocean warming, preceded massive carbon injection[11,12], and a relatively modest input of carbon (~2,500 Gt) exceptionally depleted in ^{13}C (<−50‰) is suggested by globally examined carbon isotope and carbonate dissolution records[15]. However, this explanation necessarily implies that a large amount (probably ~5,000 Gt or more) of ^{13}C-depleted carbon was stored as gas hydrate and free gas during the late Palaeocene[6].

The amount of carbon in present-day gas hydrate is poorly constrained, but probably <10,000 Gt (refs 5,16,17). Significantly warmer ocean bottom waters during the latest Palaeocene (~9 °C; ref. 1) would necessarily mean thinner gas hydrate stability zones (GHSZs) along continental margins[7]. Some authors have suggested this implies much less gas hydrate than the present, so that dissociation of gas hydrates cannot explain the carbon inputs of the hyperthermals[16–18]. However, a possible alternative is that a large amount of gas hydrate was held in a relatively small volume of sediment when T_{sf} was 5–9 °C above that of the present for millions of years[5]. We address this idea here.

Several one-dimensional (1D) models have been developed to simulate gas hydrate formation in marine sediment columns over long time intervals[8,19,20]. In general, organic matter lands on the sea floor and is buried through a GHSZ where microbes convert organic matter to CH_4; gas hydrate then precipitates when CH_4 concentrations surpass its solubility within the GHSZ. The thickness of the GHSZ is determined by salinity, pressure and temperature profiles in sediment. The amount and distribution of gas hydrate within the GHSZ, however, depend on several factors, in particular the organic carbon content that escapes oxidation in shallow sediment, the reaction rate of methanogenesis, the sedimentation rate, fluid advection, CH_4 diffusion, and time. Although heterogeneities are not considered in 1D models, when the simulations are run over millions of years, they give reasonable first-order depth profiles of gas hydrate at multiple locations, such as Blake Ridge and the Cascadia margin[8,19,20].

[1]Department of Chemical & Biomolecular Engineering, Rice University, Houston, Texas 77005, USA, [2]Department of Earth Sciences, Rice University, Houston, Texas 77005, USA, [3]Institutionen för Geologiska Vetenskaper, Stockholms Universitet, Stockholm 106 91, Sweden, [4]College of Oceanic and Atmospheric Sciences, Oregon State University, Corvallis, Oregon 97331, USA. †Present address: Shell International Exploration and Production, Houston, Texas 77082, USA. *e-mail: gg2@rice.edu; jerry@rice.edu.

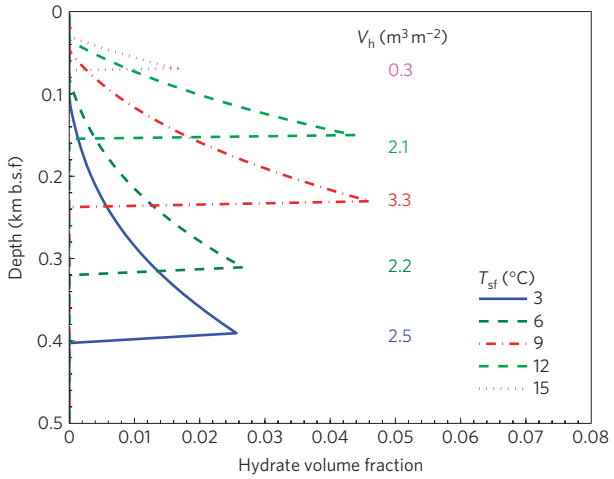

Figure 1 | The gas hydrate volume fraction ($V_{frac,h} \equiv S_h\phi$) with respect to depth below the sea floor at different seafloor temperatures T_{sf} (Case I). $D_{sf} = 2.0$ km. The total gas hydrate volume per unit seafloor area (V_h, in m^3 m^{-2}) is given for each curve. For the parameters see Supplementary Table S2. Note that changes in V_h are not straightforward because temperature impacts multiple parameters (Supplementary Table S2).

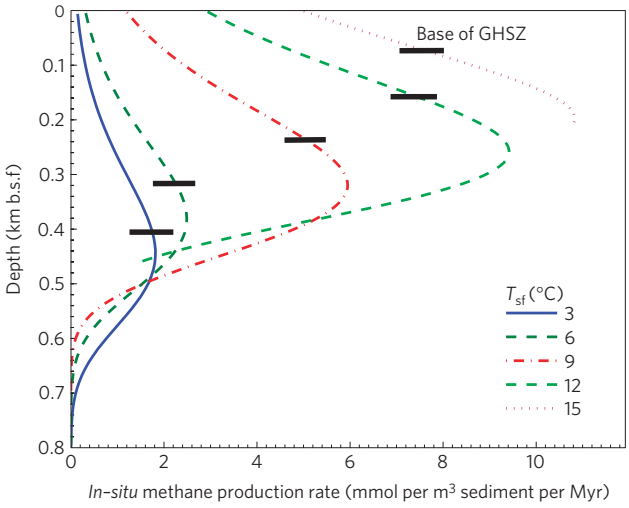

Figure 2 | Methane production profiles with respect to depth below the sea floor at different seafloor temperatures (Case I). $D_{sf} = 2.0$ km. The effects of higher organic carbon input and elevated methanogenesis rates at higher sediment temperatures have been included. The black bars show the base of the GHSZ for each T_{sf}. The parameters (Supplementary Table S2) are the same as those in Fig. 1.

We provide two initial sets of simulations for gas hydrate distribution below the sea floor (Fig. 1 and Supplementary Fig. S3a) using a 1D model[8] with parameters given in the Supplementary Information. These sets pertain to hypothetical locations where the water depth is 1 or 2 km, and where the bottom-water temperature is between 3 and 15 °C. Parameters were chosen so that a 'base case' (2 km; 3 °C) has conditions analogous to those on the present-day outer Blake ridge, an extensive region well known for investigations of gas hydrate[21] (Methods and Supplementary Information).

Most simulations render a generic shape for the amount and distribution of gas hydrate below the sea floor (Fig. 1). At some shallow depth (~25 to 100 m below sea floor, m.b.s.f.), the methane concentration surpasses the gas hydrate solubility condition, and hydrate begins to accumulate. The amount then increases with depth such that sediment contains 1–7% gas hydrate (v/v) at the base of the GHSZ. The depth profile of gas hydrate abundance for the 'base case' is fairly similar to that for sites on the outer Blake ridge. In fact, if all parameters are adjusted to that of Ocean Drilling Program site 997, the ensuing profile gives a good representation of the overall gas hydrate distribution at this location[8,21].

As emphasized above and elsewhere[7,16,17], warmer bottom water significantly impacts the thickness of the GHSZ on medium to long ($>10^3$ yr) timescales (Fig. 1). These changes occur because warmer bottom water increases sub-seafloor temperatures, and this affects the depth of the triple point of gas hydrate, dissolved gas and free gas[7,8]. The overall effect is to raise the base of the GHSZ, and to thin its thickness.

At elevated T_{sf} on the million-year timescale, however, increased amounts of hydrate may occur within the GHSZ (Fig. 1) for two reasons. First, a change of T_{sf} from 3 to 9 °C results in a decrease in dissolved [O_2] at the sea floor, which increases the flux of organic carbon that escapes oxidation in the water column and shallow sediment[24] (Methods and Supplementary Information), and which enters the GHSZ (ref. 17). The organic carbon content just below the sea floor (α_0) can increase by a factor of 1.7 to 6, depending on water depth, organic carbon rain and other factors (Supplementary Fig. S2). Second, when T_{sf} rises from 3 to 9 °C, the methanogenesis rate constant within the GHSZ increases. Between 0 and 40 °C, this increase is exponential with a factor of 2.5 to 3.0 (Supplementary Fig. S1) for several known methanogens[25–28] (Methods and Supplementary Information). Thus, methane production at a given depth within the GHSZ can be enhanced by several fold, and the zone of maximum methanogenesis moves closer to the sea floor (Fig. 2). Whereas temperature changes affect other parameters, such as CH_4 diffusion rates, they do not impact hydrate distribution very much.

Elevated seafloor temperature thins the GHSZ but increases CH_4 production within this zone (Fig. 2). The combination of both shortens the time to attain steady state and affects the total volume of gas hydrate beneath a unit area of sea floor (V_h). Our simulations demonstrate that, with all other parameters similar except for the increased T_{sf} and corresponding amount of organic carbon landing on the sea floor and rate of methanogenesis, some sites on the sea floor can have greater amounts of gas hydrate beneath bottom waters at T_{sf} of 9 °C than at 3 °C. As an example (Case I), for water depth D_{sf} = 2 km, V_h increases from 2.5 m^3 m^{-2} at T_{sf} of 3 °C to 3.3 m^3 m^{-2} at 9 °C (Fig. 1). This can also happen at shallower water depths (Case II, $D_{sf} = 1$ km; Supplementary Fig. S3a).

An important issue is whether these are a few cases resulting from specific parameters or from more general solutions. Previous work has shown that key parameters affecting gas hydrate distribution in marine sediment can be scaled into dimensionless groups[8]. This enables results from countless potential simulations with different specific parameters to be examined collectively. Two primary dimensionless groups are: $Pe_1/\overline{Da}$, the ratio of sedimentation rate to average reaction rate; and $N_{t\phi}$, the ratio of GHSZ thickness L_t to the characteristic compaction length L_ϕ (ref. 8 and Supplementary Information.)

The total hydrate volume per unit seafloor area at a bottom-water temperature of 9 °C can be compared with that at 3 °C as a ratio $k = V_{h,9C}/V_{h,3C}$. This ratio depends on the water depth and T_{sf} (Fig. 2 and Supplementary Fig. S3). It also varies with organic carbon rain and dissolved [O_2] at 3 °C (Supplementary Fig. S3), because these impact α_0 (Supplementary Fig. S2 and ref. 24). At 2 km water depth, $k > 1.0$ is likely for many circumstances because α_0 can easily increase by a factor of 2 when T_{sf} rises from 3 to 9 °C (Fig. 3 and Supplementary Fig. S2b). At 1 km depth, $k > 1.0$ is also possible, although this requires α_0 to increase by a factor of 5 when T_{sf} rose from 3 to 9 °C (Supplementary Fig. S2a). Greater gas hydrate amounts with T_{sf} of 9 °C ($k > 1.0$) generally occur for systems characterized by low $Pe_1/\overline{Da}$ and low $N_{t\phi}$ (Fig. 3). These are

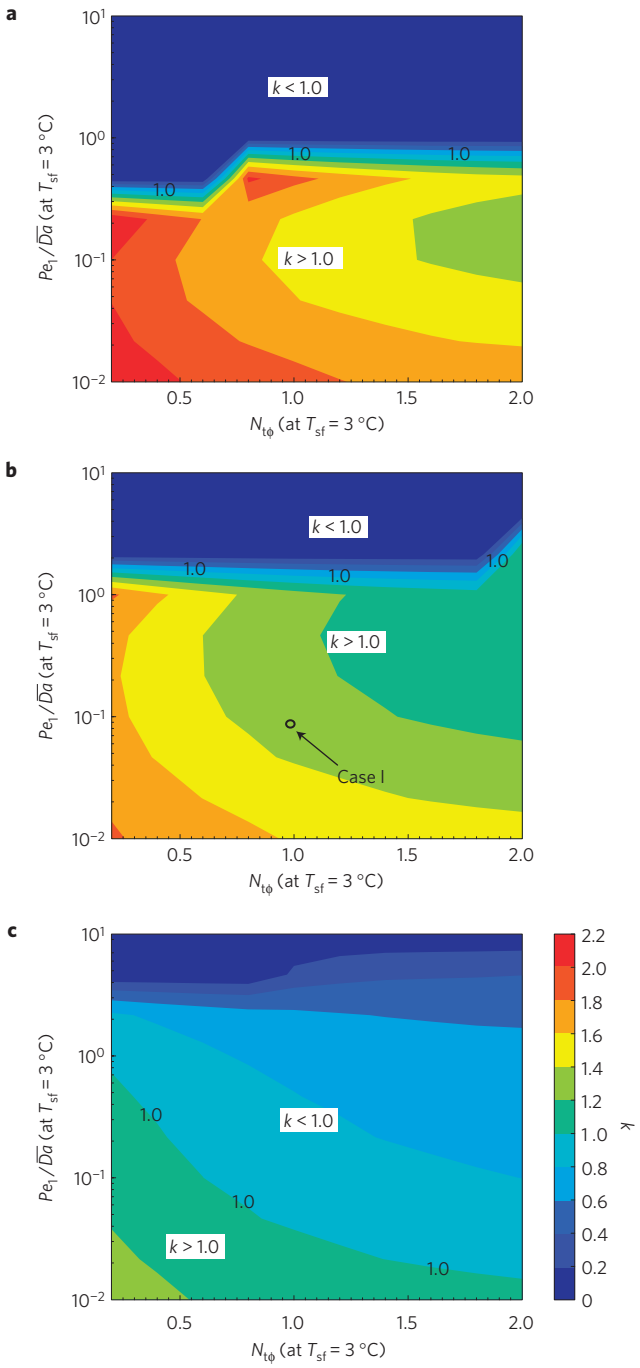

Figure 3 | Contour plots showing the ratio of total hydrate volume at seafloor temperature (T_{sf}) of 9 °C to that at 3 °C ($k = V_{h,9C}/V_{h,3C}$). **a**–**c**, Organic carbon rain (μmol cm^{-2} yr^{-1}): 10 (**a**), 30 (**b**), 100 (**c**). $k > 1$ means that the total gas hydrate volume is greater with warmer deep ocean water. Case I is that shown in Fig. 1. $(Pe_1/\overline{Da})_{3C}$ represents the ratio of sediment burial to average reaction rate at $T_{sf} = 3$ °C; $N_{t\phi,3C}$ represents the ratio of the GHSZ thickness at $T_{sf} = 3$ °C to the characteristic length of compaction. Seafloor depth $D_{sf} = 2.0$ km. For other system parameters see Supplementary Table S3.

locations, such as the present-day Blake ridge, where modest to high amounts of solid organic matter move relatively slowly through the GHSZ at deeper water depth.

Although concentrated deposits of gas hydrate dominated by focused fluid flow have received considerable attention, most of the total gas hydrate reservoir probably occurs disseminated in sediment over large regions such as the outer Blake ridge. These systems, where microbial methanogenesis of organic matter and methane diffusion lead to dispersed gas hydrate over millions of years (Fig. 1), are the type that can produce greater amounts of gas hydrate beneath the sea floor during prolonged conditions of slightly elevated deep-ocean temperature (that is, 3–6 °C warmer than the present). Interestingly, in these cases, higher amounts of gas hydrate will be shifted closer to the sea floor (Fig. 1), and faster rates of methanogenesis (Fig. 2) would recharge gas hydrate systems following methane loss more quickly.

The global abundance of marine gas hydrate at present is very large but poorly constrained[5,16,17]. Despite warmer bottom water and smaller GHSZs in the Early Palaeogene, the amount may have been similar to the present day, irrespective of the exact quantity. This is because elevated T_{sf} increases organic carbon contents entering sediment and raises methanogenesis rates. Furthermore, gas hydrate would have been more susceptible to repeated discharges of CH_4 owing to shallower occurrence within the GHSZ, and would have recharged faster after a CH_4 release because of enhanced methane production. These last predictions are intriguing because they are consistent with generic interpretations of global carbon isotope ($\delta^{13}C$) records during the Early Palaeogene[1,6,9,10].

Methods

The mathematical model and numerical algorithm for our simulations have been detailed in previous work[8]. All factors affecting gas hydrate formation over time are the same in each simulation, except those that depend on water depth and T_{sf} (see Supplementary Information). We make the following four assumptions. First, a change in T_{sf} at a given location implies a corresponding change in sea surface temperature where the water initially sank. Second, at a higher sea surface temperature, dissolved [O_2] at surface waters, which equals O_2 solubility, decreases[22]. Third, there are general relationships between dissolved [O_2] and water depth[23]; there are also relationships between organic carbon rain and dissolved [O_2] and the fraction of organic carbon rain buried in sediment[24]. Fourth, the methanogenesis rate constant λ increases with temperature significantly[25–28], and follows the Arrhenius equation $\lambda = A\exp(-E/RT)$, where T is temperature, E is the activation energy, R is the gas constant and A is a constant (see Supplementary Information). The first three assumptions imply that, when T_{sf} increases, organic carbon content just below the sea floor (α_0) increases because of decreased dissolved [O_2]. Each simulation was conducted so that steady state was reached, which generally occurred after tens of millions of years.

Received 18 May 2011; accepted 30 September 2011; published online 6 November 2011

References

1. Zachos, J. C., Dickens, G. R. & Zeebe, R. E. An early Cenozoic perspective on greenhouse warming and carbon-cycle dynamics. *Nature* **451,** 279–283 (2008).
2. Lourens, L. J. *et al.* Astronomical pacing of late Palaeocene to early Eocene global warming events. *Nature* **435,** 1083–1087 (2005).
3. Nicolo, M. J., Dickens, G. R., Hollis, C. J. & Zachos, J. C. Multiple early Eocene hyperthermals: Their sedimentary expression on the New Zealand continental margin and in the deep sea. *Geology* **35,** 699–702 (2007).
4. Stap, L. *et al.* High-resolution deep-sea carbon and oxygen isotope records of Eocene thermal maximum 2 and H2. *Geology* **38,** 607–610 (2010).
5. Dickens, G. R. Down the rabbit hole: Toward appropriate discussion of methane release from gas hydrate systems during the Paleocene–Eocene thermal maximum and other past hyperthermal events. *Clim. Past* **7,** 1139–1174 (2011).
6. Dickens, G. R. Rethinking the global carbon cycle with a large, dynamic and microbially mediated gas hydrate capacitor. *Earth Planet. Sci. Lett.* **213,** 169–182 (2003).
7. Dickens, G. R. The potential volume of oceanic methane hydrates with variable external conditions. *Org. Geochem.* **32,** 1132–1193 (2001).
8. Bhatnagar, G., Chapman, W. G., Dickens, G. R., Dugan, B. & Hirasaki, G. J. Generalization of gas hydrate distribution and saturation in marine sediments by scaling of thermodynamic and transport processes. *Am. J. Sci.* **307,** 861–900 (2007).
9. Tripati, A. & Elderfield, H. Deep-Sea temperature and circulation changes at the Paleocene–Eocene thermal maximum. *Science* **308,** 1894–1898 (2005).

10. Sluijs, A. *et al*. Subtropical Arctic Ocean temperatures during the Palaeocene/Eocene thermal maximum. *Nature* **441,** 610–613 (2006).
11. Thomas, D. J., Zachos, J. C., Bralower, T. J., Thomas, E. & Bohaty, S. Warming the fuel for the fire: Evidence for the thermal dissociation of methane hydrate during the Paleocene–Eocene thermal maximum. *Geology* **30,** 1067–1070 (2002).
12. Sluijs, A. *et al*. Environmental precursors to rapid light carbon injection at the Palaeocene/Eocene boundary. *Nature* **450,** 1218–1221 (2007).
13. Zeebe, R. E. & Zachos, J. C. Reversed deep-sea carbonate ion gradient during Paleocene–Eocene thermal maximum. *Paleoceanography* **22,** PA3201 (2007).
14. Kvenvolden, K. A. Methane hydrate—a major reservoir of carbon in the shallow geosphere? *Chem. Geol.* **71,** 41–51 (1988).
15. Zeebe, R. E., Zachos, J. C. & Dickens, G. R. Carbon dioxide forcing alone insufficient to explain Palaeocene–Eocene thermal maximum warming. *Nature Geosci.* **2,** 576–580 (2009).
16. Milkov, A. V. Global estimates of hydrate-bound gas in marine sediments: how much is really out there? *Earth Sci. Rev.* **66,** 183–197 (2004).
17. Buffett, B. & Archer, D. Global inventory of methane clathrate: Sensitivity to changes in the deep ocean. *Earth Planet. Sci. Lett.* **227,** 185–199 (2004).
18. Pagani, M., Calderia, K., Archer, D. & Zachos, J. C. An ancient carbon mystery. *Science* **314,** 1556–1557 (2006).
19. Davie, M. K. & Buffett, B. A. A numerical model for the formation of gas hydrate below the seafloor. *J. Geophys. Res.* **106,** 497–514 (2001).
20. Garg, S. K., Pritchett, J. W., Katoh, A., Baba, K. & Fujii, T. A mathematical model for the formation and dissociation of methane hydrates in the marine environment. *J. Geophys. Res.* **113,** B01201 (2008).
21. Paull, C. K. & Matsumoto, R. Leg 164 overview. *Proc. ODP Sci. Res.* **164,** 3–10 (2000).
22. Weiss, R. F. The solubility of nitrogen, oxygen and argon in water and seawater. *Deep-Sea Res.* **17,** 721–735 (1970).
23. Matear, R. J. & Hirst, A. C. Long-term changes in dissolved oxygen concentrations in the ocean caused by protracted global warming. *Glob. Biogeochem. Cycles* **17,** 1125 (2003).
24. Archer, D. E., Morford, J. L. & Emerson, S. R. A model of suboxic sedimentary diagenesis suitable for automatic tuning and gridded global domains. *Glob. Biogeochem. Cycles* **16,** 17.1–17.24 (2002).
25. Zeikus, J. G. & Winfrey, M. R. Temperature limitations of methanogenesis in aquatic sediments. *Appl. Environ. Microbiol.* **31,** 99–107 (1976).
26. Price, P. B. & Sowers, T. Temperature dependence of metabolic rates for microbial growth, maintenance, and survival. *Proc. Natl Acad. Sci. USA* **101,** 4631–4636 (2004).
27. Mikucki, J. A., Liu, Y., Delwiche, M. E., Colwell, F. S. & Boone, D. R. Isolation of a methanogen from deep marine sediments that contain methane hydrates, and description of *Methanoculleus submarinus* sp. nov. *Appl. Environ. Microbiol.* **69,** 3311–3316 (2003).
28. Boone, D. R., Whitman, W. B. & Rouviere, P. in *Methanogenesis: Ecology, Physiology, Biochemistry and Genetics* (ed. Ferry, J. G.) 35–80 (Chapman Hall, 1993).

Acknowledgements

The authors thank the US Department of Energy for financial support (under Award No. DE-AC07-05ID14517 and No. DE-FC26-06NT42960).

Author contributions

G.R.D. conceived the overarching hypothesis; G.B. constructed a prototype numerical model published elsewhere with insights from G.J.H, W.G.C. and G.R.D.; G.G. modified the model for this work, carried out the simulations and prepared the data, with advice and input from G.J.H, G.R.D. and W.G.C.; G.G. and G.R.D. wrote the initial manuscript; all authors contributed to subsequent revisions.

Additional information

The authors declare no competing financial interests. Supplementary information accompanies this paper on www.nature.com/naturegeoscience. Reprints and permissions information is available online at http://www.nature.com/reprints. Correspondence and requests for materials should be addressed to G.G. or G.R.D.